PREPARATION AND EVALUATION OF ANTICANCER POTENTIAL OF LYCOPENE LOADED NANOLIPOSOMES

Ashu Saini[1], Neeraj Sethi[2*]

[1]Department of Biochemistry, Om Sterling Global University, Hisar

[2]Department of Biotechnology, Om Sterling Global University, Hisar

saini.ashu099@gmail.com

20neerajsethi@gmail.com

*Corresponding author email; 20neerajsethi@gmail.com

Abstract

A triterpene found in nature called Lycopene exhibits strong anticancer properties. But because of its weak bioavailability, it has a low solubility in aqueous phase. To administer Lycopene with improved solubility and bioavailability, liposomal nano formulation is a viable approach. In the current study, Lycopene nanoliposomes were created, and their physical and chemical characteristics were studied and adjusted. With a particle size range of 48-135 nm, a zeta potential of -25.1 mV, and a percent entrapment effectiveness of 68.7%, Lycopene nanoliposomes showed the best characteristics for use in drug delivery applications. The ability of Lycopene loaded liposomal nano formulation to inhibit cancer cell proliferation was demonstrated by its cytotoxic efficacy against the A-549, MCF-7, and Hela cell lines. As a result, the current research effort showed how Lycopene nanoliposomes could be used as a promising nano formulation for cancer treatment.

Keywords: Nanoliposomes, Lycopene, Liposomal Nano formulation, Cancer therapy.

Introduction

The anticancer medications must be delivered to their molecular targets for chemotherapy to be effective. The therapeutic efficacy of the anticancer medicine is reduced by its random and non-targeted circulation inside the biological system. Additionally, it increases the risk of toxicity and

unfavorable side effects. Entrapping an anticancer agent in a specific carrier is a key strategy for site-specific drug administration and to minimize its negative effects. However, placing an appropriate agent on the particle's surface and guaranteeing its biocompatibility are required for carrier-mediated medication delivery to cancer sites [1].

Nanotechnology has the potential to change how cancer is diagnosed and treated [2]. Because of the inherent drawbacks of traditional chemotherapy, several nanotechnologies have been developed and put to use to treat cancer more effectively and safely. More than 40 nanotherapeutics, including chemotherapeutic and imaging agents, have previously been administered to patients. Multiple therapeutic actions can be combined into a single platform using nanomaterials [3]. They may therefore be directed against particular tissues for this reason. A deeper comprehension of the biological aspects and physicochemical characteristics of nanotherapeutics is also necessary for effective systemic distribution of nanotherapeutics to solid tumors [4].

Nanoliposomes are well-known drug delivery methods that are non-immunogenic, biocompatible, and degradable drug carriers [5]. Another benefit of liposomal bioactive delivery is the increased bioavailability of the bioactive ingredient as it travels through the digestive tract and into the bloodstream. Hydrophilic materials may dissolve into the watery center of nanoliposomes during formulation, while hydrophobic materials may be linked to the bilayer. Therefore, both hydrophilic and hydrophobic bioactive chemicals could be used in nanoliposomes. Advanced nano-herbal products can now be developed using nanoformulations thanks to the discovery and refinement of phyto nanoformulations [6]. For the treatment of CVS problems, respiratory illnesses, diabetes, cancer, etc., several herbal drugs are employed. Nanoformulations have made it possible to improve cancer treatment, which has led to a decrease in both the severity of the disease and its mortality rates. It has been shown that the triterpenoid molecule Lycopene has anti-inflammatory [7] and hepatoprotective [8] effects. Additionally, both free carboxylic acid and the aglycone of saponins are examples of lycopene triterpenoids) [8]. In human breast cancer cell lines (Michigan Cancer Foundation-7) it modifies the glucocorticoid receptor and lowers the levels of Bcl2 (an anti-apoptotic protein) [9, 10]. Lycopene is commonly utilized in pharmaceutical formulations that may be applied locally and consumed orally because of its low degree of toxicity and natural origin [11, 12]. Such

restrictions might be circumvented by the Lycopene -loaded new liposomal nano formulation, which also offers a potential method for successfully delivering Lycopene. Lycopene nanoliposomes may offer a possible formulation with improved solubility, bioavailability, and therapeutic potential. The development, characterization, and assessment of Lycopene nanoliposomes for anti-cancer activity against cancer cell lines were done in this study.

Materials and methods

Drug and chemicals

The supplier of Lycopene was Sigma Aldrich in India. The source of the cholesterol was Molychem in Mumbai. The National Center for Cell Science (NCCS), Pune provided the cell lines A-549 (Human lung adenocarcinoma epithelial cells), MCF-7 (Human breast adenocarcinoma cells), and Hela (Human cervical carcinoma cell line), while Lecithin, Minimum Essential Eagle Medium, Foetal Bovine Serum (FBS), penicillin & streptomycin were acquired from Himedia, Mumbai. Analytical reagent grade chemicals were used in all study projects.

Preparation of Lycopene nanoliposomes

In order to create Lycopene nanoliposomes (LNLs), thin film hydration was used. The two main excipients used were lecithin and cholesterol. In a mixture of 35 ml ethanol and 65 ml carbon tetra chloride, lecithin (650 mg), cholesterol (87 mg), cetyl trimethyl ammonium chloride (18 mg), and 200 mg of Lycopene were dissolved. The mixture was evaporated in a rotary evaporator at 42 degrees for 4.5 hours in order to generate a thin lipid film. The film was then hydrated for one hour at 70 degrees Celsius with 90 ml of deionized water containing 2 ml of 0.035% Tween-80 solution. The resulting big, stable, and hydrated multilamellar vesicle suspension was then put through sonication and extrusion to finish the procedure.

Characterization of Lycopene nanoliposomes

The average particle size of the nanoliposomes and the degree of heterogeneity (polydispersity index) of size-optimized nanoliposomes were measured using dynamic light scattering. To determine if the liposomal nanoformulations is stable at 25 °C, the electrokinetic potential in a colloidal dispersion of vesicles was calculated using the Zetasizer Nano ZS-90 (Malvern Instruments, Malvern, UK). Following centrifugation at 10,000 rpm, 4 °C for 30 min, the quantity of unbound medication in the supernatant was evaluated and the % encapsulation

efficiency was calculated. With the help of a transmission electron microscope (TEM-Hitachi-H-7501SSP/N-817-0520, Japan), the morphological evaluation of the improved batch was carried out. In order to acquire a TEM micrograph, one drop of optimized LNLs was originally put onto a copper grid, air-dried, and scanned at 60,000 magnification factor and 80,000 V accelerating voltage. Before extrusion, the morphology of LNLs was examined using a fluorescent photomicroscope at a 100X magnification (LEICA DM 2500 M). Using the FTIR spectrophotometer Affinity-1 (Shimadzu, Japan), the KBr pellet of powdered samples of Lycopene, lecithin, cholesterol, and LNLs was examined in the range of 4500-500 cm^{-1}. TGA/DSC 3+ Stare System, Mettler Toledo AG, Analytical, Switzerland was used to conduct a differential scanning calorimetry-thermogravimetric analysis (DSC-TGA) examination of LNLs and dummy nanoparticles in order to ascertain the physical characteristics of the drug and liposomes. Using an alumina pan and a heat flow rate of 15 C/min, samples (5 mg) were scanned between 30 and 500 C.

In vitro release profile of Lycopene nanoliposomes

The dialysis sac method was used to analyze the release profile. LNLs (10 mg) were retained in a dialysis sac and placed in a solution of ethanol (25%) and phosphate buffer (0.1 M) saline with a pH of 7.4 while being swirled continuously at 90 rpm at a constant temperature of 37 °C. At regular intervals of 1, 2, 3, 6, 12, and 24 hours, one ml samples were taken out and collected. They were then analyzed by HPLC (Agilent 1200 Infinity Series) using a ZORBAX SB C-18 column (5 m, 150 x 4.6 mm) and a mobile phase made up of acetonitrile: water (75:25 v/v), 216 nm, and 8.24 min.

Antioxidant activity

The antioxidant activity was calculated as an indicator of the ability of antioxidants to scavenge DPPH. Pure Lycopene and LNLs were incubated for 30 minutes in the dark with 1, 1-diphenyl-2-picrylhydrazyl (DPPH), a free radical that was dissolved in methanol (3.9 mg/100 ml). At 517 nm, a UV spectrophotometer was used to measure the absorption. The inhibition of DPPH was assessed using Blank nanoliposomes (Negative control), Lycopene (Positive control), and LNLs. The proportion of DPPH inhibition by pure Lycopene and Lycopene loaded nanoliposomes was calculated using the equation shown below.

Percent antioxidant activity = (Control Abs.) - (Sample Abs.)   X   100

(Control Abs.)

In-vitro cytotoxic assay

By using the MTT test on the three cell lines A-549 (Human lung adenocarcinoma epithelial cells), MCF-7 (Human breast adenocarcinoma cells), and Hela (Human cervical carcinoma cell line), the in vitro cytotoxicity activity of LNLs solutions was assessed. To assess the cytotoxic or cytostatic effect of a therapeutic bioactive agent or hazardous compounds, tetrazolium dye-based tests are used. Since the MTT reagent is typically photosensitive, experiments are typically carried out in a dark environment [11]. Cell lines (both healthy and cancerous) were grown in medium supplemented with 10% inactivated FBS, 100 l/ml streptomycin, and 100 l/ml penicillin, and then incubated at 370C and 5% CO2 in a humidifier incubator. The cells were sub cultured in a 0.25% trypsin solution under sterile conditions after reaching 70% confluence. Compound and standard stock solutions were made in DMSO (M/ml), and subsequent dilutions (1 M, 10 M, 20 M, 50 m, and 100 m per ml) were made in the medium in 96-well plates. Based on the features of each cell line's proliferation, the density of each was calculated. After an initial 8-hour incubation, triplicate wells were treated for three days with varied LNL concentrations (0.1-1000 g/ml) and Lycopene. Three days later, 3 l of MTT solution (5 mg/ml) was added to the medium. The incubation period was 180 minutes, and the results were based on the mitochondrial conversion of 3-(4, 5-dimethylthiazol-2-yl) 2,5-diphenyltetrazolium bromide (MTT) The entire relative percent of metabolically active cells was compared to Formazan crystals and untreated controls. Formazan crystals were dissolved in DMSO, and the microplate reader (BIORAD) was used to measure the absorbance at 570 nm. Using Lycopene as a reference medication, the anticancer efficacy of synthetic compounds was evaluated.

Results and Discussion

Synthesis of Lycopene Nanoliposomes (LNLs)

The creation of Lycopene nanoliposomes involved the thin film hydration process. Nanoliposomes can be used for the trapping, distribution, and release of both lipid and water-soluble molecules since they contain both lipid and aqueous phases. Following its absorption into

Research paper   ,

the liposomes, the hydrophobic medication Lycopene's pharmacological profile generally improved in the current investigation.

Characterization of Lycopene Nanoliposomes

Particle size analysis and Zeta potential

Liposomal nanocarriers have a significant property called particle size. It impacts cellular absorption, drug release profile, encapsulation effectiveness, and bio-distribution [12,13]. A specific size of nanoliposome (150 nm) can leave or enter the cancer cells' microenvironment. The malignant cells are more vascular and larger in size [14]. Vascular mediators will consequently build up at the tumor sites. However, the enhanced permeability & retention (EPR) impact of high molecular weight therapies is made possible by the leaky vasculature of cancer cells. Drugs encapsulated in liposomes as small as 400 nm can passively target cancer cell locations but are barred from healthy tissues by the endothelium wall [15–20]. The particle size of LNLs in the current study was determined to be 211 nm, pointing to their high vasculature and accumulation. To evaluate the connection between surface charge and stability, zeta potential calculations were performed [21–22]. Nano liposomal formulations' zeta potential can aid in regulating their fusion, precipitation, and aggregation. A larger negative number denotes a more stable preparation and more cellular absorption. LNLs were discovered to have a zeta potential of -42.5 mV, indicating greater stability.

Percent encapsulation efficiency (% EE)

By calculating the free drug concentration in the dispersion medium, the encapsulation effectiveness of the LNLs formulation was calculated. The amount of free Lycopene in the supernatant was calculated using HPLC after the suspension was centrifuged for 30 min at 10,000 rpm (4 C) (Fig. 1). The following equation is used to determine encapsulation efficiency:

$$EE(\%) = \{(C_{initial} - C_{final})/C_{initial}\} \times 100$$

Where, $C_{initial}$ - initial drug concentration

and the C_{final} - free drug measured in the supernatant after centrifugation

The percent encapsulation was found to be 65.2% for Lycopene.

Morphological studies using Photomicroscopy **and** *TEM*

Lycopene-containing multilamellar vesicles were discovered to be stable [23]. Prior to extrusion, the multilamellar vesicles were seen under a photomicroscope at a 100X magnification. An analytical method used to study very small morphological details of liposomal vesicles at the nanometric scale is the transmission electron microscope (TEM). Size of nanoparticles affects a molecule's or drug's release, solubility, and dissolution rates [24–26]. Depending on their size and form, nanoliposomes can pass through various human organs [27, 28]. It was noted that the LNLs nano formulation was separated and consistently spherical (Fig. 2). According to TEM, prepared LNLs were between 60 and 150 nm in size.

FTIR spectroscopy

Due to the strong interaction between drugs and excipients, FTIR can differentiate a wide variety of functional groups, offer data in the form of peaks or spectra that reveal structural information, and are sensitive to changes in molecular arrangement. The FTIR signal for the -OH stretch occurs at 3447 cm^{-1} and is specific to Lycopene. The FTIR peak for the -CH2 group vibrations is at 3030 cm-1. The C=O functional group is inferred by the FTIR signal at 1742 cm^{-1}. The 1318 cm^{-1} FTIR peak relate to the stretch-OH group. Stretch, or the C-O group, peaks at 1043 cm^{-1} and 1421 cm^{-1}, respectively (Fig. 3A). The FTIR signal for cholesterol is the hydroxyl group at 3512 cm^{-1}. According to Fig. 3B, the peak at 2930 cm^{-1} is due to the aromatic stretch of CH=CH, the peak at 1565 cm^{-1} is due to the carboxylic acid C=O group, and the peak at 988 cm^{-1} is due to the ester stretch. The peak of the amide group at 3546 cm^{-1} is the FTIR peak that is characteristic of lecithin. A P-O-C stretch vibration is present at 1011 cm^{-1}, a P=O stretch vibration is present at 1320 cm^{-1}, and a vibration for the -OH carboxylic stretch is present at 2989cm^{-1} (Fig. 3C).

The distinctive peaks for Lycopene, cholesterol, and lecithin may be seen in the FTIR spectrum of LNLs. Peaks for the hydroxyl group are at 3445 cm^{-1}, an aromatic stretch of CH=CH is at 3023 cm^{-1}, the carboxylic acid C=O group is at 1501 cm^{-1}, and the cholesterol ester stretch is at 909 cm^{-1} (Fig. 3D).

Amide exhibits a peak at 3021 cm^{-1}, a vibration for the -OH carboxylic stretch at 2897 cm^{-1}, a P=O stretch vibration at 1365 cm^{-1}, and a P-O-C stretch vibration at 1102 cm^{-1}. The FTIR peaks are indicative of Lycopene. The FTIR signal at 3012 cm^{-1} is for the vibrations of the -CH2 group, and the peak for the -OH group (Stretch) is at 1390 cm^{-1}. Stretch, or the C-O group, reached its climax at 965 cm^{-1} and 1300 cm^{-1}, respectively. The interaction between Lycopene and lecithin

reveals a considerable shift in P=O and P-O-C, with P=O shifting from 1338 cm^{-1}to 1387 cm^{-1} and P-O-C shifting from 988 cm^{-1}to 999 cm^{-1}.

Differential Scanning calorimetric and Thermo-gravimetric analytical studies

Two endothermic peaks could be seen on the free Lycopene DSC thermogram. The presence of Lycopene was established by the low intensity of the first endothermic peak at 286 ^{o}C, while the high intensity of the second peak indicated the substance's crystalline form (29–30). In the case of the thermogram for LNLs, an endothermic peak was seen at 375 ^{o}C, followed by the start of disintegration at 370 ^{o}C (Fig. 4A). The low intensity of the peak supported the amorphous nature of LNLs. Two endothermic peaks were seen in blank nanoliposomes: a low intensity peak at 170 ^{o}C and a second peak at 365 ^{o}C that decomposes beyond 365 ^{o}C (Fig. 4B). Due to its distinctive nature, the observed peaks were not sharp.

To ascertain the weight loss in relation to temperature, TGA was performed. Maximum weight loss in fake nanoliposomes was found at 340 ^{o}C, but maximum weight loss in LNLs occurred at 350 ^{o}C after a modest melting temperature change, suggesting a notable difference in the presence of co-amorphous phase.

In vitro drug release profile for LNLs using HPLC

The controlled rate of drug release from the nanoparticle matrix protects it against accelerated metabolism and deterioration. According to in-vitro drug release data, 85.6% of the pure form of Lycopene was released in 3 hours. However, only 38.9% Lycopene was released from the LNLs after 3 hours, which was the sustained release. 71.6% of Lycopene was freed from LNLs in 24 hours. Because Lycopene is hydrophobic (nonpolar), the drug release profile of LNLs as a whole demonstrates a continuous release of Lycopene over time. Additionally, lipid bilayers thick and strongly walled dense matrix were created by liposomal nanoformulations around the Lycopene particles, ensuring their prolonged release (Fig. 5).

Antioxidant activity

To determine the antioxidant activity of compounds that are encapsulated, the DPPH analysis is widely performed [31, 32]. The stable free radical 1,1-diphenyl-2-picrylhydrazyl has spare electrons distributed throughout the entire molecule, giving it a rich violet hue. It has a band of absorption about 517 nm [33-34]. When a DPPH solution is uniformly combined with a molecule that can donate (have an oxidizing character) an atom of hydrogen, violet color disappears. The antioxidant chemical known as Lycopene is widely used. When DPPH (a

hydrogen atom donor) was added to the Lycopene solution, a color change from violet to pale yellow could be noticed. As a result, the absorption band shrankCompared to the unencapsulated analog of free Lycopene, LNLs showed a higher percentage of DPPH inhibition. Nanoencapsulation of Lycopene by lipid bilayer results in size reduction at the nanometer scale with more exposed surface, which results in increased antioxidant activity (Fig. 6).

Anticancer activity

Using the MTT assay, the A-549, MCF-7, and Hela cell lines were used to test the Lycopene and LNLs for anticancer activity. The results are shown in Table 1. The cytotoxic effectiveness of LNLs is mostly due to the huge surface area of nanoliposomes. Smaller bilayer vesicles can more effectively penetrate the tumor's deepest layers [35–37]. The literature has already reported on Lycopene anti-cancerous properties [38]. In healthy cells, mitochondrial dehydrogenase is found. It degrades the pale yellow MTT dye's tetrazolium ring structure [39] to produce dark purple formazan crystals that are impermeable to cell membranes and build up inside of the cells [40–42]. A liposomal nanoplatform containing oleanolic acid, an isomer of Lycopene, had significant cytotoxic effects on cancer cell types via inducing apoptosis. In general, NPs loaded via mPEG-PLA/PLGA were found to be more cytotoxic to cancer cells and were therefore considered to be a more effective method of delivering oleanolic acid [43]. The results showed that LNLs exhibit a potent anticancer effect with IC50 values of 5.8 g/ml, 5.2 g/ml, and 4.9 g/ml against A-549 cells, MCF-7 cell lines, and Hela cell lines, respectively. This effect was more pronounced than that of pure BA particles, which had IC50 values of 26.66 g/ml, 25.89 g/ml, and 31.

Conclusions

Due to their advantageous effects and favorable therapeutic to toxicity ratios, phytochemicals have been successfully used for a variety of therapeutic applications. The information presented in this research showed how LNLs were prepared, characterized, optimized, and had in vitro antioxidant and anticancer properties. Due to the creation of lipid bilayer vesicles, Lycopene 's size was reduced, resulting in increased bioavailability and prolonged release of Lycopene. The therapeutic potential of Lycopene at low doses combined with improved drug residence time are made possible by the lipid-based nanoformulation. Nanoliposomes (lipid bilayer) can diffuse

bioactive substances directly inside of cells and are chemically compatible with plasma membranes. In particular, our findings showed that LNLs were more effective at fighting cancer in vitro than their structural sibling. LNLs are thus potentially useful in the fight against cancer.

Conflict of Interest

There is no conflict of interest whatever.

References

1. Peer, D., & Margalit, R. (2004). Tumor-targeted hyaluronan nanoliposomes increase the antitumor activity of liposomal doxorubicin in syngeneic and human xenograft mouse tumor models. *Neoplasia (New York, NY)*, *6*(4), 343.

2. Preiss, M. R., & Bothun, G. D. (2011). Stimuli-responsive liposome-nanoparticle assemblies. *Expert opinion on drug delivery*, *8*(8), 1025-1040..

3. Schroeder, A., Heller, D. A., Winslow, M. M., Dahlman, J. E., Pratt, G. W., Langer, R., & Anderson, D. G. (2012). Treating metastatic cancer with nanotechnology. *Nature Reviews Cancer*, *12*(1), 39.

4. Shi, J., Kantoff, P. W., Wooster, R., & Farokhzad, O. C. (2017). Cancer nanomedicine: progress, challenges and opportunities. *Nature Reviews Cancer*, *17*(1), 20.

5. Zamboni, W. C. (2005). Liposomal, nanoparticle, and conjugated formulations of anticancer agents. *Clinical cancer research*, *11*(23), 8230-8234.

6. Allen, T. M., & Cullis, P. R. (2013). Liposomal drug delivery systems: from concept to clinical applications. *Advanced drug delivery reviews*, *65*(1), 36-48.

7. de los Reyes, C., Zbakh, H., Motilva, V., & Zubía, E. (2013). Antioxidant and anti-inflammatory meroterpenoids from the brown alga Cystoseira usneoides. *Journal of natural products*, *76*(4), 621-629.

8. Yogeeswari, P., & Sriram, D. (2005). Sethi, N., Bhardwaj, P., Kumar, S., & Dilbaghi, N. (2019). Development and Evaluation of Ursolic Acid Co-Delivered Tamoxifen Loaded Dammar Gum Nanoparticles to Combat Cancer. *Advanced Science, Engineering and Medicine*, *11*(11), 1115-1124.

9. Sethi, N., Bhardwaj, P., Kumar, S., & Dilbaghi, N. (2019). Development And Evaluation Of Ursolic Acid Loaded Eudragit-E Nanocarrier For Cancer Therapy. *International Journal of Pharmaceutical Research (09752366)*, *11*(2)..

Research paper

10. Saneja, A., Kumar, R., Singh, A., Dubey, R. D., Mintoo, M. J., Singh, G., ... & Gupta, P. N. (2017). Development and evaluation of long-circulating nanoparticles loaded with betulinic acid for improved anti-tumor efficacy. *International journal of pharmaceutics*, *531*(1), 153-166.

11. Vivek, V., Sethi, N., & Kaura, S. (2022). Green synthesis and evaluation of antibacterial activity of zinc nanoparticles from Calotropis procera leaves..

12. Danaei, M., Dehghankhold, M., Ataei, S., Hasanzadeh Davarani, F., Javanmard, R., Dokhani, A., & Mozafari, M. (2018). Impact of particle size and polydispersity index on the clinical applications of lipidic nanocarrier systems. *Pharmaceutics*, *10*(2), 57.

13. Blasi, P., Giovagnoli, S., Schoubben, A., Ricci, M., & Rossi, C. (2007). Solid lipid nanoparticles for targeted brain drug delivery. *Advanced drug delivery reviews*, *59*(6), 454-477.

14. Kaura, S., Parle, M., Insa, R., Yadav, B. S., & Sethi, N. (2022). Neuroprotective effect of goat milk. *Small Ruminant Research*, *214*, 106748..

15. Dhanda, P., Sura, S., Lathar, S., Shoekand, N., Partishtha, H., & Sethi, N. (2022). Traditional, phytochemical, and biological aspects of Indian spider plant..

16. De Leo, V., Maurelli, A. M., Giotta, L., & Catucci, L. (2022). Liposomes containing nanoparticles: preparation and applications. *Colloids and Surfaces B: Biointerfaces*, 112737.

17. Hussein, H. A., & Abdullah, M. A. (2022). Novel drug delivery systems based on silver nanoparticles, hyaluronic acid, lipid nanoparticles and liposomes for cancer treatment. *Applied Nanoscience*, *12*(11), 3071-3096.

18. Song, J. W., Liu, Y. S., Guo, Y. R., Zhong, W. X., Guo, Y. P., & Guo, L. (2022). Nano–liposomes double loaded with curcumin and tetrandrine: preparation, characterization, hepatotoxicity and anti–tumor effects. *International Journal of Molecular Sciences*, *23*(12), 6858.

19. Sethi, N., Kaura, S., Dilbaghi, N., Parle, M., & Pal, M. (2014). Garlic: A pungent wonder from nature. *International research journal of pharmacy*, *5*(7), 523-529..

20. Shekunov, B. Y., Chattopadhyay, P., Tong, H. H., & Chow, A. H. (2007). Particle size analysis in pharmaceutics: principles, methods and applications. *Pharmaceutical research*, *24*(2), 203-227.

21. Hunter, R. J. (2013). *Zeta potential in colloid science: principles and applications* (Vol. 2). Academic press.

22. Aswathy, M., Vijayan, A., Daimary, U. D., Girisa, S., Radhakrishnan, K. V., & Kunnumakkara, A. B. (2022). Betulinic acid: A natural promising anticancer drug, current situation, and future perspectives. *Journal of Biochemical and Molecular Toxicology*, e23206.

23. Singh, A., Vengurlekar, P. R. E. R. A. N. A., & Rathod, S. (2014). Design, development and characterization of liposomal neem gel. *Int J Pharm Sci Res*, *5*, 140-148.

24. Al-Jamal, W. T., & Kostarelos, K. (2007). Liposome–nanoparticle hybrids for multimodal diagnostic and therapeutic applications.

25. Albanese, A., Tang, P. S., & Chan, W. C. (2012). The effect of nanoparticle size, shape, and surface chemistry on biological systems. *Annual review of biomedical engineering*, *14*, 1-16.

26. Kaur, H., Ahuja, M., Kumar, S., & Dilbaghi, N. (2012). Carboxymethyl tamarind kernel polysaccharide nanoparticles for ophthalmic drug delivery. *International journal of biological macromolecules*, *50*(3), 833-839.

27. Danaei, M., Dehghankhold, M., Ataei, S., Hasanzadeh Davarani, F., Javanmard, R., Dokhani, A., ... & Mozafari, M. (2018). Impact of particle size and polydispersity index on the clinical applications of lipidic nanocarrier systems. *Pharmaceutics*, *10*(2), 57.

28. Geze, A., Putaux, J. L., Choisnard, L., Jehan, P., & Wouessidjewe, D. (2004). Long-term shelf stability of amphiphilic β-cyclodextrin nanosphere suspensions monitored by dynamic light scattering and cryo-transmission electron microscopy. *Journal of microencapsulation*, *21*(6), 607-613.

29. Fontanay, S., Kedzierewicz, F., Duval, R. E., & Clarot, I. (2012). Physicochemical and thermodynamic characterization of hydroxy pentacyclic triterpenoic acid/γ-cyclodextrin inclusion complexes. *Journal of Inclusion Phenomena and Macrocyclic Chemistry*, *73*(1-4), 341-347.

30. Chen, X., Lu, S., Gong, F., Sui, X., Liu, T., & Wang, T. (2022). Research on the synthesis of nanoparticles of Lycopene and their targeting antitumor activity. Journal of Biomedical Materials Research Part B: Applied Biomaterials.

31. Molyneux, P. (2004). The use of the stable free radical diphenylpicrylhydrazyl (DPPH) for estimating antioxidant activity. *Songklanakarin J. Sci. Technol*, *26*(2), 211-219.

32. Kumar, Rakesh, Neeraj Sethi, and Sushila Kaura. "Bio-processing and analysis of mixed fruit wine manufactured using Aegle marmelos and Phoenix dactylifer." (2022)..

33. Kong, B., Zhang, H., & Xiong, Y. L. (2010). Antioxidant activity of spice extracts in a liposome system and in cooked pork patties and the possible mode of action. *Meat science*, *85*(4), 772-778.

34. Castan, L., del Toro, G., Fernández, A. A., González, M., Ortíz, E., & Lobo, D. (2013). Biological activity of liposomal vanillin. *Journal of medicinal food*, *16*(6), 551-557.

35. Fujiwara, Y., Takeya, M., & Komohara, Y. (2014). A novel strategy for inducing the antitumor effects of triterpenoid compounds: blocking the protumoral functions of tumor-associated macrophages via STAT3 inhibition. *BioMed research international*, *2014*.

36. Mosmann, T. (1983). Rapid colorimetric assay for cellular growth and survival: application to proliferation and cytotoxicity assays. *Journal of immunological methods*, *65*(1-2), 55-63.

37. de Pace, R. C. C., Liu, X., Sun, M., Nie, S., Zhang, J., Cai, Q., & Wang, S. (2013). Anticancer activities of (−)-epigallocatechin-3-gallate encapsulated nanoliposomes in MCF7 breast cancer cells. *Journal of liposome research*, *23*(3), 187-196.

38. Ma, J., Guan, R., Shen, H., Lu, F., Xiao, C., Liu, M., & Kang, T. (2013). Comparison of anticancer activity between lactoferrin nanoliposome and lactoferrin in Caco-2 cells in vitro. *Food and chemical toxicology*, *59*, 72-77.

39. Gerlier, D., & Thomasset, N. (1986). Use of MTT colorimetric assay to measure cell activation. *Journal of immunological methods*, *94*(1-2), 57-63.

40. V. Meerloo, J., Kaspers, G. J., & Cloos, J. (2011). Cell sensitivity assays: the MTT assay. In *Cancer cell culture* (pp. 237-245). Humana Press.

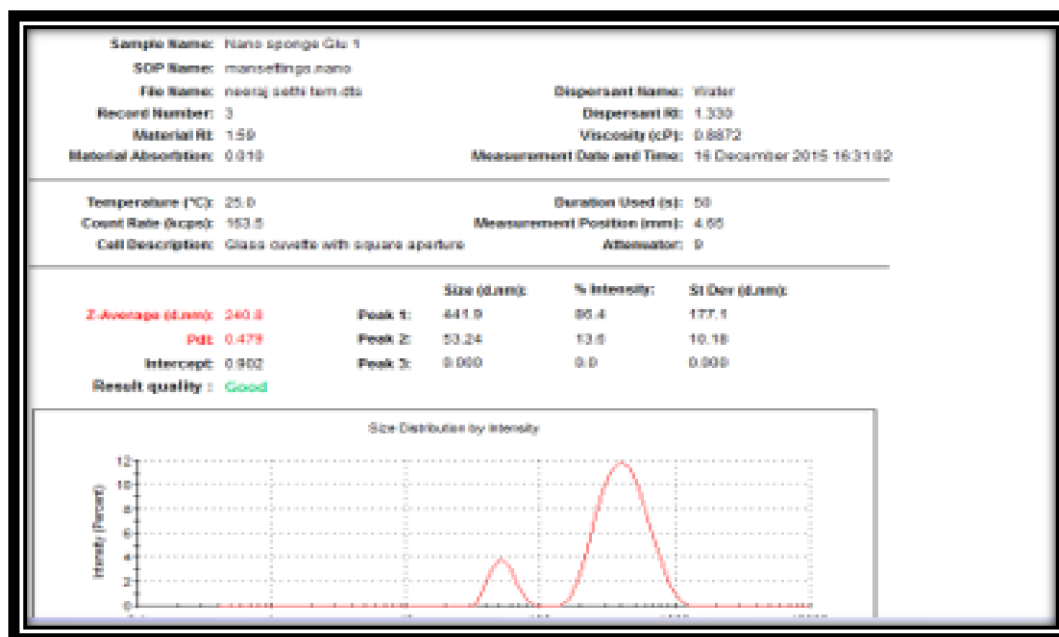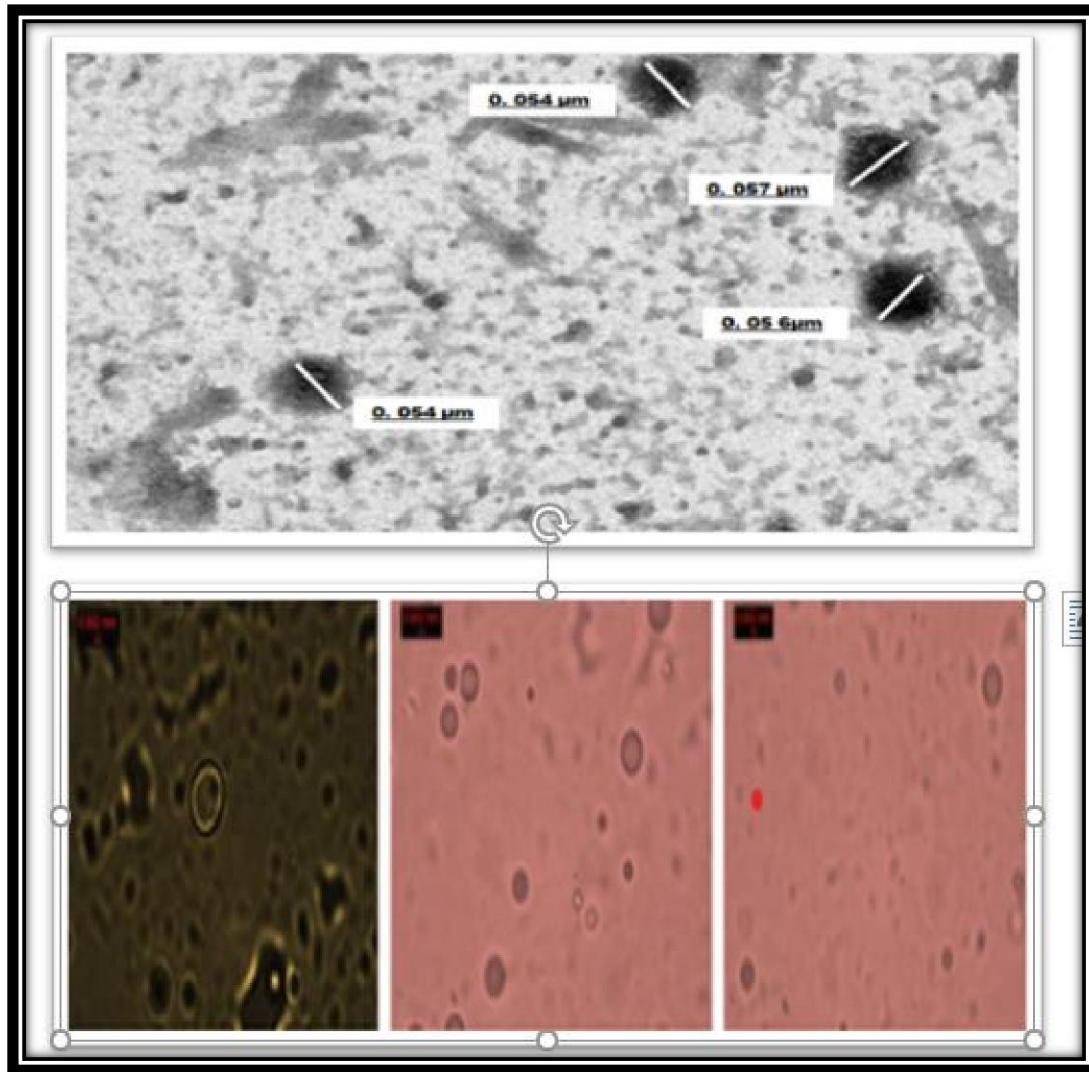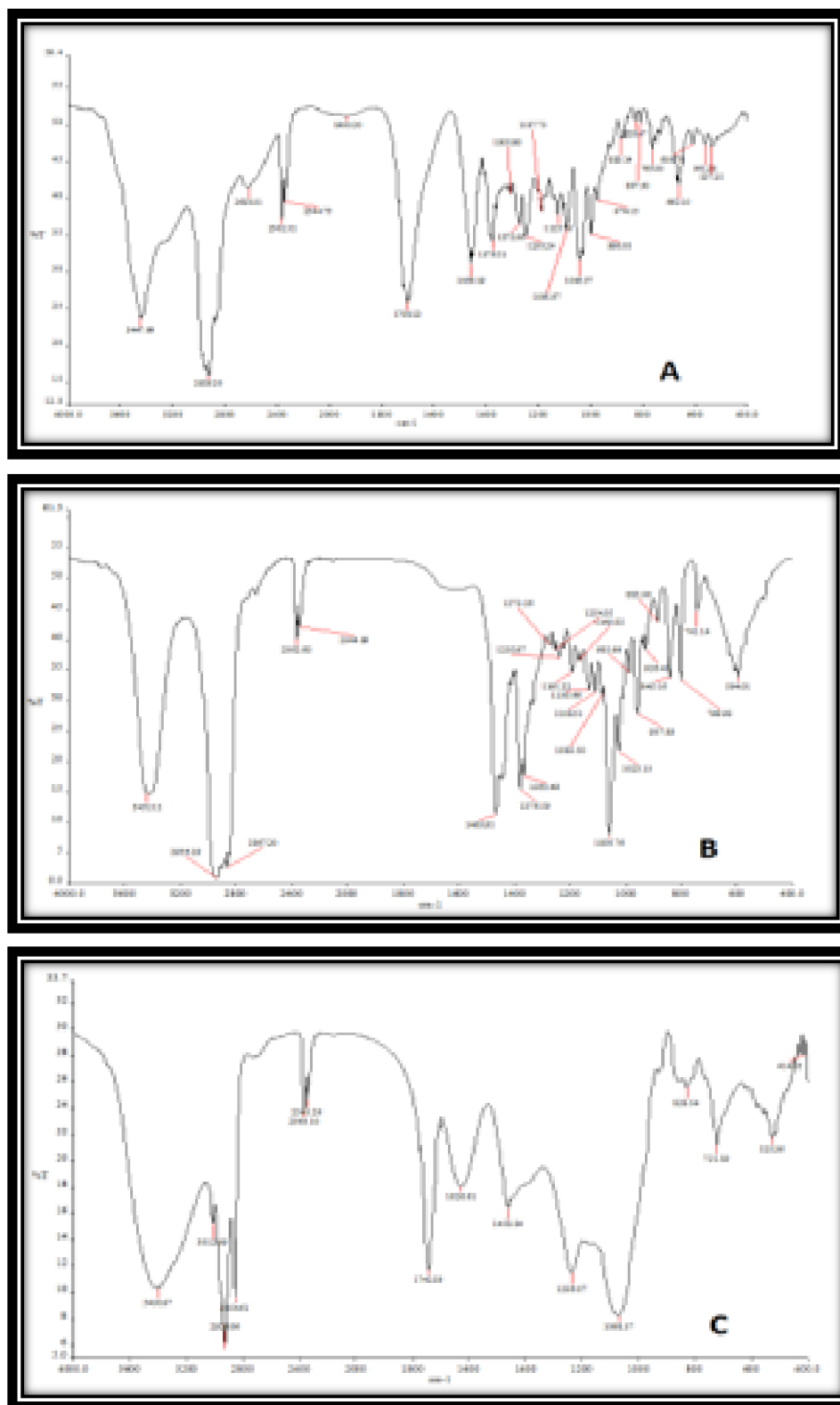**Figure 1: Zeta potential of Lycopene loaded nanoliposomes**

Figure 2: TEM and Photo microscopic images of Lycopene loaded nanoliposomes

Research paper © 2012 IJFANS. All Rights Reserved, UGC CARE Listed (Group -I) Journal Volume 12, Iss 03, 2023

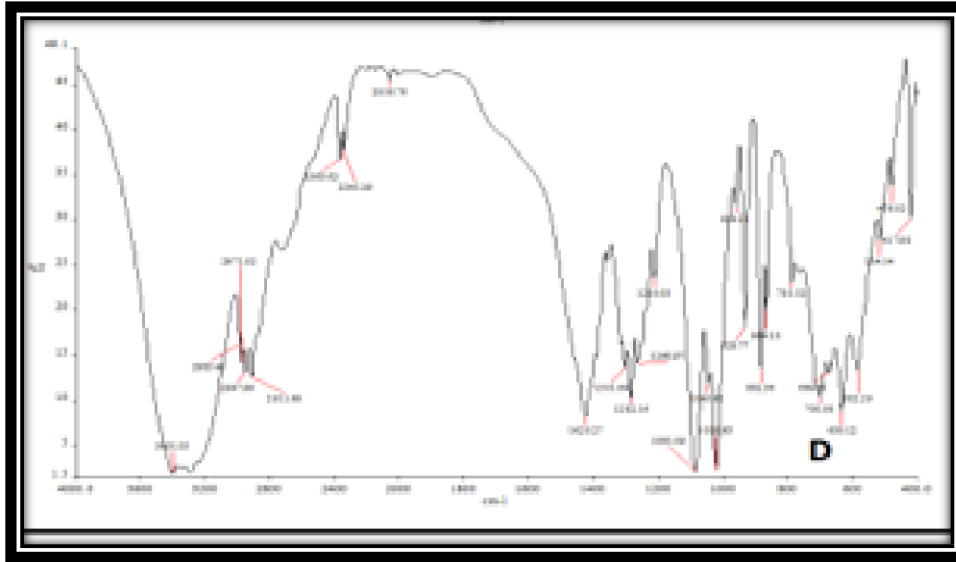**Figure3. FTIR spectra of (A) Lycopene, (B) Cholesterol, (C) Lecithin, (D) Lycopene loaded liposomal nanoformulations**

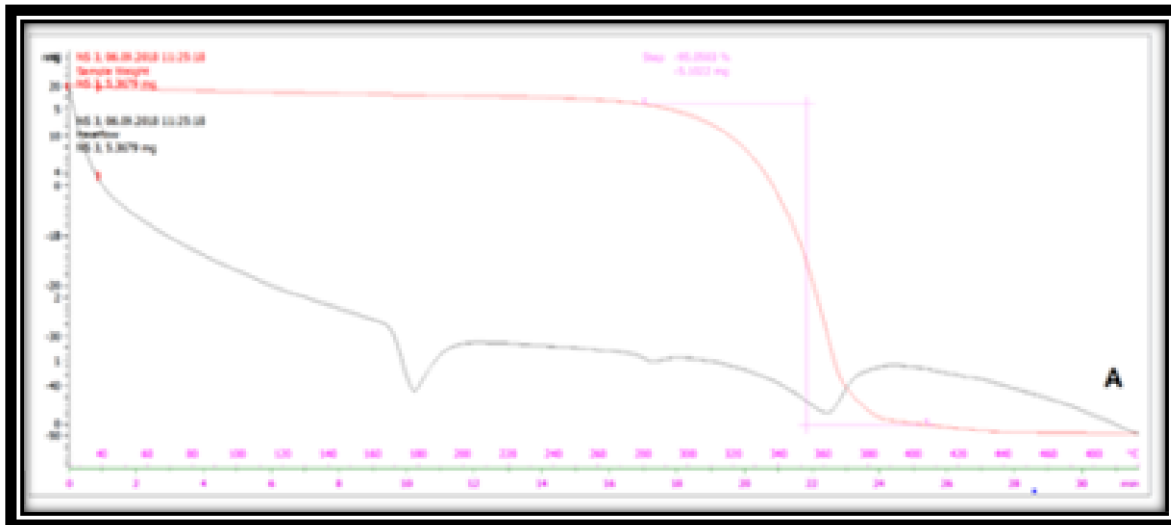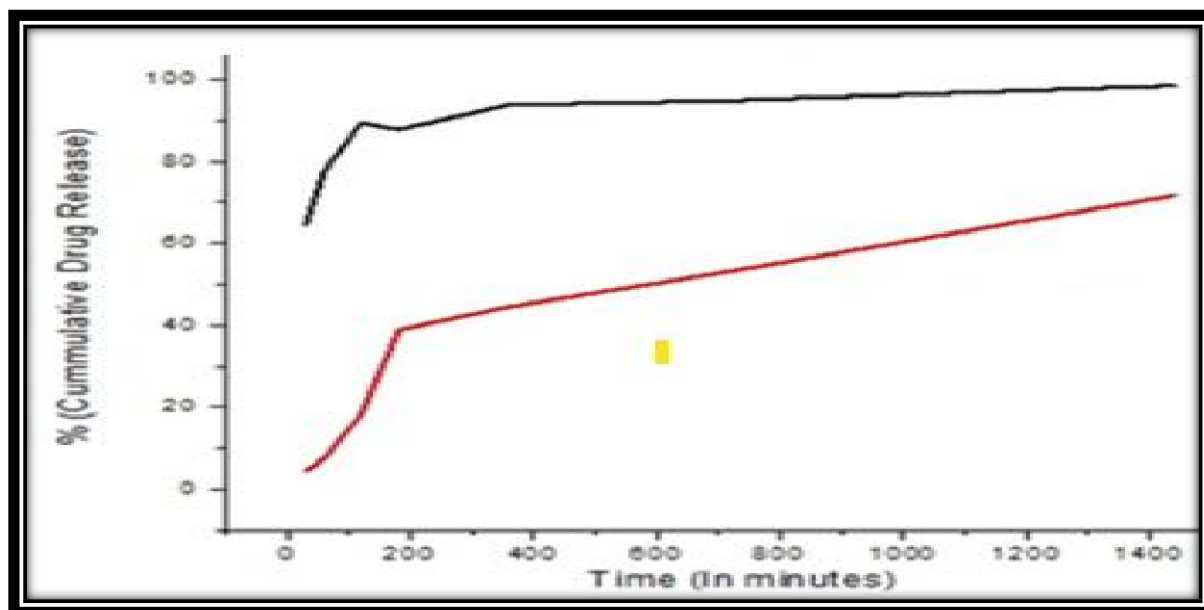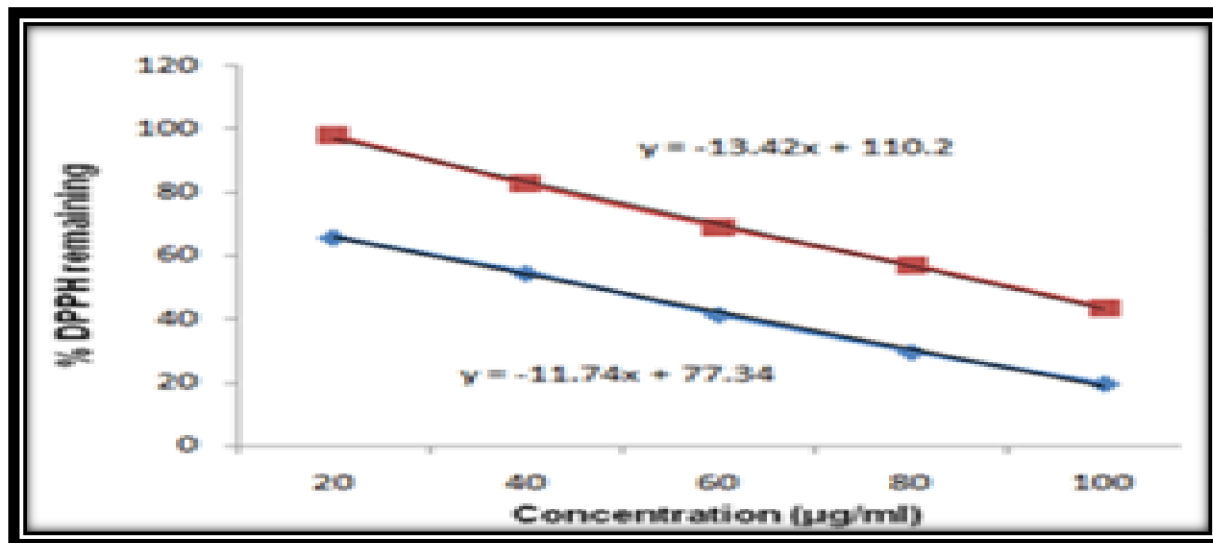**Figure 4. DSC of Lycopene loaded liposomal nanoformulations (A).**

Figure 5. *In vitro* **drug release of Lycopene nanoliposomes**

Figure 6. Antioxidant activity of Lycopene nanoliposomes

Table 1: IC50 values of LNPs along with pure drug Lycopene

Sample code	A-549		MCF-7		Hela	
	IC50	pIC50	IC50	pIC50	IC50	pIC50

Lycopene	28.42	1.5663	26.34	-1.4913	30.98	-1.51132
LNLs	6.3	-0.84345	6.1	-0.7480	4.8	-0.6812

Figure 7. Percentage cell inhibition of LNLs on MCF-7, A-549 and MCF-7 Cell lines after 24 h.